Available online at www.sciencedirect.com

ScienceDirect

Proceedings of the Combustion Institute 36 (2017) 3263–3270

Proceedings of the Combustion Institute

www.elsevier.com/locate/proci

Investigation of firebrand production during prescribed fires conducted in a pine forest

Alexander Filkov [a,b,*], Sergey Prohanov [b], Eric Mueller [c], Denis Kasymov [b], Pavel Martynov [b], Mohamad El Houssami [c], Jan Thomas [c], Nicholas Skowronski [d,e], Bret Butler [f], Michael Gallagher [d,e], Kenneth Clark [d,e], William Mell [g], Robert Kremens [h], Rory M. Hadden [c], Albert Simeoni [i]

[a] *School of Ecosystem and Forest Sciences, University of Melbourne, 4 Water St, Creswick, VIC 3363, Australia*
[b] *National Research Tomsk State University, Department of Physical and Computational Mechanics, 36 Lenin av, Tomsk 634050, Russia*
[c] *School of Engineering, University of Edinburgh, King's Buildings, Mayfield Road, Edinburgh EH9 3JL, UK*
[d] *USDA Forest Service, Northern Research Station, 180 Canfield St, Morgantown, WV 26505, USA*
[e] *USDA Forest Service, Northern Research Station, 501 Four Mile Road, New Lisbon, NJ 08064, USA*
[f] *USDA Forest Service, Rocky Mountain Research Station, 5775 W US Highway 10, Missoula, MT 59808, USA*
[g] *USDA Forest Service, Pacific Wildland Fire Sciences Laboratory, 400 N 34th St., Suite 201, Seattle, WA 98103, USA*
[h] *Rochester Institute of Technology, Center for Imaging Science, 54 Lomb Memorial Drive, Rochester, NY 14623, USA*
[i] *Exponent, Inc. 9 Strathmore Road, Natick, MA 01760, USA*

Received 4 December 2015; accepted 17 June 2016
Available online 28 September 2016

Abstract

This paper represents a study on the characterization of firebrand production which was carried out, using experimental fires conducted as prescribed fires in the New Jersey Pine Barrens, USA in March of 2013–2015. Several preliminary techniques were tested to characterize the firebrand production. Firebrands were collected from three plots for each year and analyzed for mass and size distribution. Thermal imagery was used to measure the velocity, size and number of firebrands in 2014 and 2015. The distribution of firebrands was evaluated in a monitored volume during the experiment. It was found that not less than 70% of collected particles were bark fragments and the rest were pine and shrub branches. The number of firebrands decreases with increasing the cross section area of firebrands. The mass of the particles varied from 5 to 50 mg, and the maximum number of the particles was observed for the mass range of 10–20 mg. About 80% of firebrands were particles with the cross section area of (5–20) $\times$ 10^{-5} m^2. These results are consistent with the available

* Corresponding author at: School of Ecosystem and Forest Sciences, University of Melbourne, 4 Water St, Creswick, VIC 3363, Australia.
E-mail address: alexander.filkov@unimelb.edu.au (A. Filkov).

http://dx.doi.org/10.1016/j.proci.2016.06.125

observations of real fires [1,2]. Processing of infrared video showed that starting from a distance of 13 m from fire front, an increasing number of firebrands were observed in a controlled volume, increasing in number up to 180 per second. Relationships describing the time-variation of the number of particles that dropped on a 1.4 m^2 surface and the number of particles that flew through a 1 m^3 volume were obtained. Comparing the experimental and calculated data, we can conclude that these relationships allow us to describe the two numbers with an acceptable accuracy (adj. R^2 0.74 and 0.86, respectively). In addition, the velocity of the particles, which depended on the wind velocity, was in the 0.1–10.5 m/s range, with an average value of 2.5 m/s.

Keywords: Surface fire; Firebrands; Generation; Characteristics

1. Introduction

Spot fires are generally recognized as being an important and complex problem in the context of the prediction of forest fire propagation. They can be a threat for fire fighters and other persons which have to deal with forest fires. Observing the propagation of real spot fires, it is very difficult to appreciate when and where a spot fire can occur. The phenomenon can occur in any fuel type, but is usually initiated in natural fuels with natural (e.g., lightning strikes) or manmade (e.g., campfires, runaway prescribed fires, downed or arcing powerlines, arson) origins.

The ignition of structures in a Wildland-Urban Interface (WUI) community is caused by the exposure of heat fluxes from flame or firebrands generated by a wildfire. Firebrands are generated due to combustion of trees and buildings during fires in such territories. The probability of ignition is dependent both on physical properties (e.g., type of fuels) and fire exposure conditions (e.g., extent and duration of the heat flux from flames and firebrands).

Firebrands are entrained by the wind in the atmosphere [3–4] and can be transported over long distances. Hot firebrands may ignite fuels, far from direct heat flux from the fire, resulting in fire propagation. The flow of firebrands generated in WUI fires may ignite vegetation and mulch located near houses and buildings [5]. This, in turn, can lead to ignition of neighboring houses and buildings. Understanding the ignition mechanisms of fuel beds and structures, due to firebrand exposure, is important for the development of a new generation of mathematical models of for predicting and preventing the propagation of fires in populated areas [6].

Ignition of fuels due to firebrand exposure has been insufficiently investigated, but a limited number of laboratory studies are available in the literature [7]. Understanding how firebrands can ignite surrounding fuel beds is an important consideration in mitigating the fire propagation in communities [6]. In addition, the size distribution of firebrands produced during the combustion of vegetation and structures is relatively unknown under field conditions [8]. Past firebrand studies did not assess the effect of firebrands on the spread rate of the fire front, as well as the characteristics of their generation. In particular, there is a need to estimate the size of the particles generated under field conditions and their characteristics such as the velocity and the temperature. Based on these measurements, it is necessary to obtain the characteristics of their formation depending on the type of fuels, the weather conditions and the fire intensity. A major achievement in WUI fire research would be the development of a model to predict the generation of firebrands during the burning of vegetation and structures, the subsequent transport in the atmosphere, and the final ignitability of materials due to the firebrand exposure [7]. Therefore, a study on the characterization of firebrand production was carried out, using experimental fires conducted as prescribed fires in the New Jersey Pine Barrens, USA in March of 2013, 2014 and 2015.

2. Methods

2.1. Plots and equipment description

The experiment was conducted in the Pinelands National Reserve in southern New Jersey (USA). It included a series of full-scale experiments in 2013 (EX1), 2014 (EX2) and 2015 (EX3), respectively. The area of the experimental sites was varied from 4.3 (EX2) to 6.7 (EX1 and EX3) ha (Fig. 1).

It should be noted that EX3 was conducted again at the same site as EX1. The forest type for the both blocks was pitch-pine scrub-oak, dominated in the canopy by pitch pine, with intermittent clusters of post-oak and white oak in the subcanopy. The understory contained a shrub layer of huckleberry, blueberry, and scrub oaks.

In all cases, the burns were carried out in early March, before the initiation of 'green-up', or the growth of new vegetation in the spring. Both fires were ignited in a line, by drip torch, along the northern-most road (~330 m and ~207 m long, respectively). The lines were continuously drawn out from east to west.

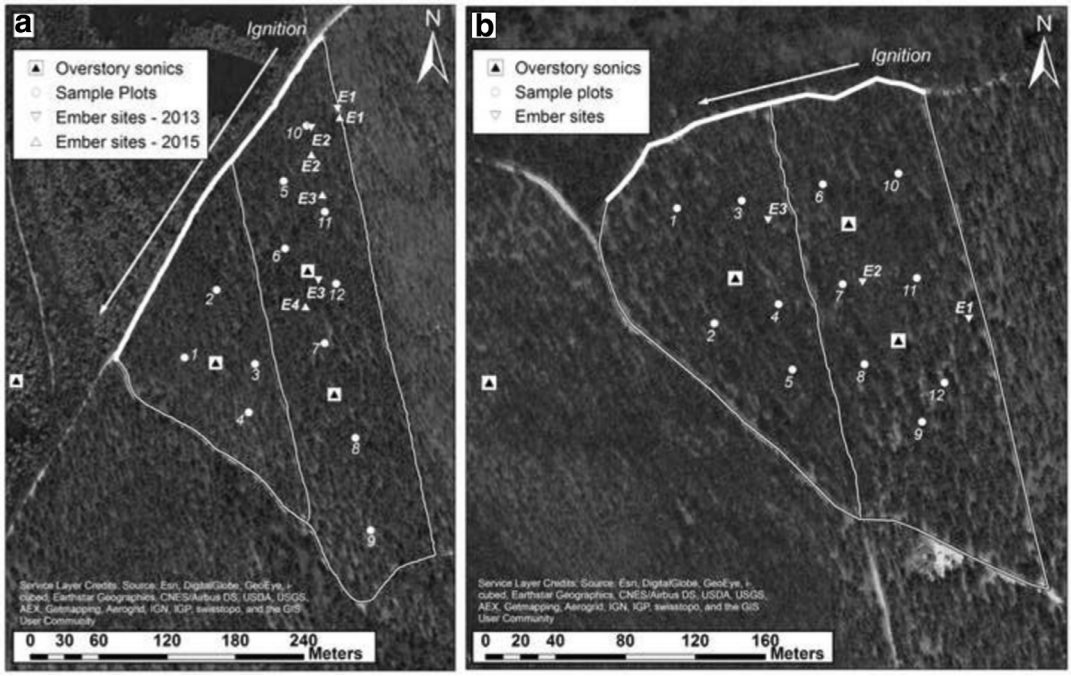

Fig. 1. Location of four overstory towers, 12 plots for collection of fuels and 3 plots for collection of firebrands for EX1, EX3 (a) and EX2 (b).

Four 12.5 m tall overstory towers and twelve understory towers were set on the experimental sites (Fig. 1). Tower locations within the block were selected so as to reduce any directional bias and clustering of measurements, allowing for flexible choice of an ignition line, given the conditions leading up to the burn. One overstory tower was located outside of each block, to the west, in order to monitor the ambient conditions throughout the course of the fire. The choice of 12.5 m corresponded to roughly canopy height. The sensors, installed in the overstory towers, included 3D sonic anemometers (RM 80,001 V, R. M. Young Co.) which provided measurements of wind velocity, turbulence, and air temperature.

Before each experiment, destructive sampling of the forest floor and shrub layer was carried out in 1 m^2 clip plots [9]. Three clip plots were selected within each of 12 larger 20 m × 20 m sites, centered at the locations indicated in Fig. 1 (around of each of 12 understory towers). This destructive sampling technique was repeated after the fire (using an additional three clip plots per site), and consumption was estimated by comparing the measurements.

A time history of the fire progression was recorded from an aircraft using Rochester Institute of Technology's Wildfire Airborne Sensor Program (WASP) [8,10]. The WASP provided time-stamped, othomosaiced, and georeferenced long-wave infrared (8.0–9.2 μm) and visible (0.4–0.9 μm) spectral band images, at a resolution of 640×512. In addition, a number of digital and analog cameras were placed within the sites.

The thermal imagers FLIR A325 and Mikron 7600PRO were used for the diagnostics of firebrands and their characteristics on the Plot 1 EX2 and EX3. FLIR A325 operated in the range of 7.5–13 microns and Mikron 7600PRO operated in the range of 8–14 microns. Both thermal imagers recorded a video with a frequency of 30 Hz. Figure 2 shows the arrangement of equipment in EX2.

To record the particles in the air flow, the screen was installed in front of the thermal imagers. The screen was a 2.5×1.5 m gypsum wall board installed perpendicular to the underlying surface and coated with black heat-resistant paint. More details related to the experimental methods can be found in [8].

2.2. Firebrand collection

We used the same methodology for firebrand collection as in [8]. Fire resistant gypsum boards were placed on the ground at three sites in EX1, EX2 and EX3. 20 aluminum pans, 0.3×0.24 m each were positioned on each board to form a rectangle with a total cross section area of 1.4 m^2. Wire nets were placed inside the pans to allow easy extraction of captured firebrands. Pans were filled with

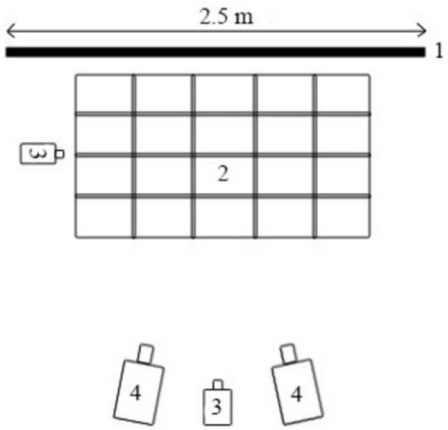

Fig. 2. Arrangement of thermal imagers: 1 – screen 2 – plot for the collection of particles, 3 – video cameras, 4 – thermal imagers.

water to extinguish captured burning particles. Plot 1 was placed near the track, delimiting the experimental parcel (Fig. 1), Plot 2 and Plot 3 were placed near understory towers. In EX1, only Plot 2 pans were covered by a thin plastic film. In EX2, all pans were covered by plastic film. Laboratory experiments showed that holes burnt in the film allowed the location and approximate size of particles to be determined. However, analysis of video from EX2 showed that some small and light firebrands can bounce and be blown away from the film. Therefore, in EX3 each plot had pans with and without film.

2.3. IR data processing

To analyze the recorded thermograms, the following method was developed. The data from «SEQ» format (file from the FLIR A325 thermal imager) were exported to the MATLAB format by using the FLIR ThermaCAM Researcher software. As a result, a set of files was received to provide the number of the test frames, the recording time up to the millisecond, and a matrix containing the temperature at each point of space.

The IR video processing task was to search for the location of flying particles, determine the temperatures and sizes and calculate the number of the particles which dropped on the surface under study. The most difficult step in the data processing is to build the track of the particle, that is, to find the place where the particle moved in the next frame. In the case where 30–50 particles appear in the frame (Fig. 3), it is difficult to determine the position of the particle in the next frame.

Therefore, a particle detector was developed to determine the location of specific particles. The detector functions by viewing the frame data and providing the coordinates of the rectangles (detections) which contain particles. After detection of all particles in the frame the particle tracker was developed.

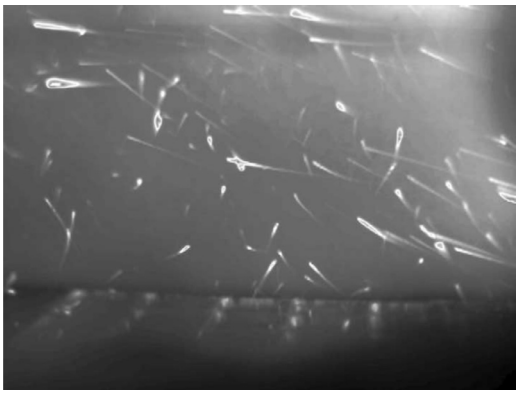

Fig. 3. Thermogram.

To determine the temperature of the particle, it is necessary to find the maximum value of the temperature in the frame limited to the rectangle of detection. Also, it is necessary to determine whether the particle is in a pan, the boundaries of which are defined in the configuration file. For this purpose, the last detection is used. If detection is within a specified quadrangle, then the particle is registered as being in a pan, and the counter of collected particles increases by one.

The software creates a video file that contains all the detection areas marked, the identification numbers of the particles, the frame number, and minimum and maximum temperatures in the frame. More detailed information is recorded in a xml-file.

3. Results and discussion

3.1. Collection analysis

It should be noted that the combustion intensity varies, depending on the year of the experiment conducted, as well as the location of the experimental plot within a site. In the 2015 EX3 experiment, the loading of fine surface fuels (needles + 1 h wood + 1 h shrub stems) was reduced as a result of the 2013 EX1 fire (whole block average in 2015 was 0.83 kg/m^2 compared to 1.37 and 1.68 kg/m^2 for EX1 and EX2, respectively), with a lower proportion in the shrub layer compared to previous years. The resulting consumption was lower as well (block average of 0.45 kg/m^2), with 54% (67% and 72% for EX1 and EX2, respectively) of the average load being consumed. Combined with drastically lower spread rates, the fire intensity in 2015 was not sufficient to generate measurable quantities of embers. More details related to the analysis of the fire behavior can be found in [8].

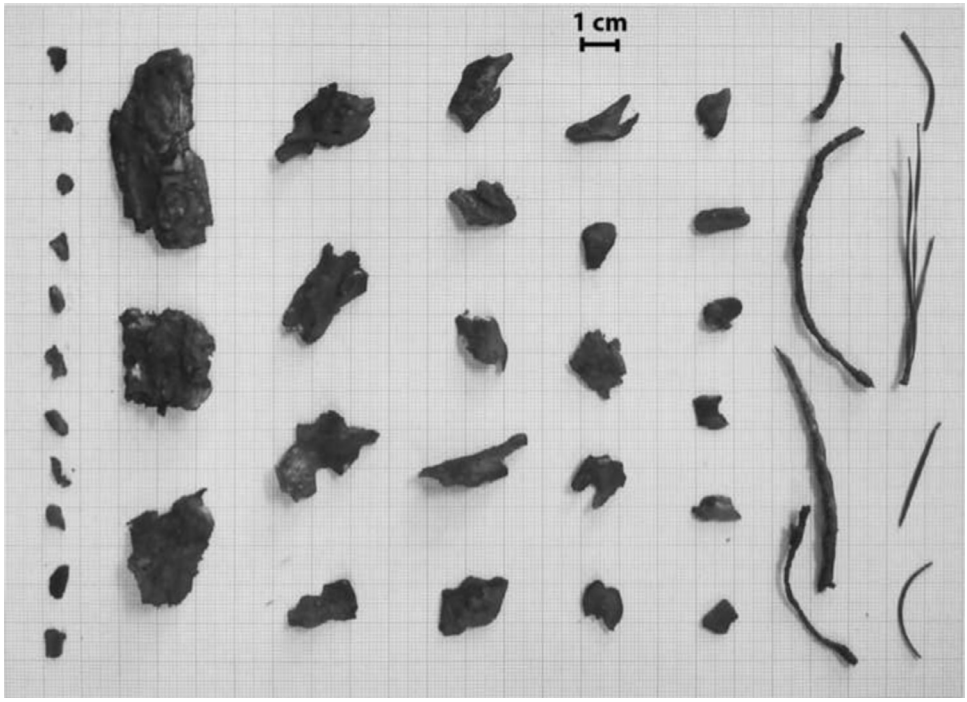

Fig. 4. Firebrands samples collected on the plots in EX1.

The collected firebrands were dried at 80 °C in an oven until reaching a constant weight, then weighed on a laboratory balance with a precision of 0.1 mg, taking into account only particles with a mass greater than 5 mg. Particle dimensions (length, width, and thickness) were measured in EX1 using an electronic caliper ($\pm 10^{-5}$ m). 5 particles were measured ten times and the systematic measurement error (difference between the mean value and maximum or minimum value) was no more than 6%. In EX2 and EX3 another technique was used to measure particle dimensions. For these particles, the area was determined using MATLAB code that calculated the total area of the particle from individual photographs. A reference length was defined in every photograph by drawing a 1 cm line in the paper where the embers were photographed, and the total area is calculated by the number of pixels that the ember occupies in the picture. The software has a precision of 4.84×10^{-5} m^2. Particles smaller than 5×10^{-3} m were discarded. Figure 4 shows firebrand samples collected from the experiment.

Table 1 shows the amount of the particles collected on the plots, depending on their type.

It should be noted that most particles were bark slices and the rest were pine and shrub branches. An exception is Plot 1 for EX2.

The mass and area distribution for each particle for all plots is shown in Fig. 5.

A substantially higher number of particles were collected in Plot 2 from EX2. This can be attributed to the fact that this plot was on the downwind edge of an area with more intense fire behavior, which included passive crowning (compared with the predominantly surface fire behavior observed elsewhere). Additionally, video footage revealed that the passage of this intense fire melted

Table 1
Quantity and percentage of collected firebrands (>5 mg and $>5 \times 10^{-3}$ m) in each plot and its corresponding density.

Firebrands	EX1			EX2		
	Plot 1	Plot 2	Plot 3	Plot 1	Plot 2	Plot 3
Total amount	83	61	333	17	1343	54
Branches (%)	15	30	11	70	31	28
Bark (%)	85	70	89	30	69	72
Density (pcs./m^2)	60	44	238	12	960	39

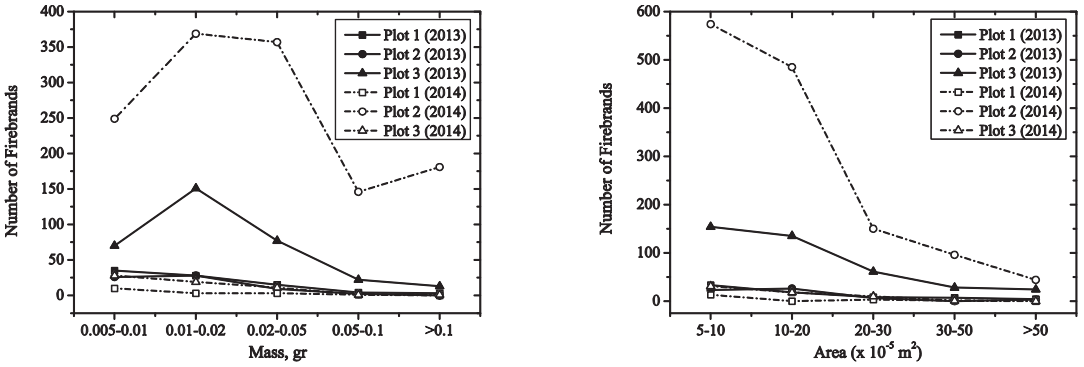

Fig. 5. Firebrands distribution for different mass ranges and area.

Table 2
Comparison between the amount of flying particles q and the relative measurement errors δ.

Frames	Program data (pcs.)	Expert 1 (pcs.)	δ (%)	Expert 2 (pcs.)	δ (%)	Expert 3 (pcs.)	δ (%)
1800–2250	61	69	12	67	9	65	6
3200–3650	41	46	12	43	5	41	0
4100–4400	31	33	6	32	3	33	6

the plastic film, allowing the deposition of more particles.

The majority of firebrands weighed between 5 and 20 mg, and the maximum number of the particles was observed for the range of 10–20 mg. A size analysis of firebrands shows that the majority (42−76%) were particles with a cross section area of (5–10) $\times$ 10^{-5} m^2. Cross sectional areas are estimated in EX1 by considering bark pieces as rectangles and branches as cylinders. About 80% of all particles had a cross sectional area in the range of (0–20) $\times$10^{-5} m^2. These findings are in agreement with the case study findings of the Angora fire [1] where more than 85% of holes that firebrands had made on trampolines were measured at less than 50 $\times$ 10^{-5} m^2.

3.2. IR video analysis

To verify the accuracy of the software, three time intervals were selected to most accurately estimate the number of flying particles. The selected intervals were as follows: 1800–2250, 3200–3650 and 4100–4400 frames. Three independent experts counted the number of flying particles not knowing the results provided by the software. The relative measurement errors were calculated according to the data. The average value of the measurement data obtained by the experts was used as the exact value. The data obtained are provided in Table 2.

Table 2 shows that the maximum relative error does not exceed 12% for the selected intervals. However, it should be noted, that there are the intervals in the video where the number of the particles is very large, and the video frame rate does not allow us to detect the whole trajectory of the particle. Working with these frames is complicated both for the program and for the person. Therefore, the error of the program operation can be significantly increased on these plots.

Due to the calibration that was chosen for the IR cameras, the maximum temperature was limited to 147 °C. This did not allow us to measure temperatures for all firebrands but it was the best way to detect most firebrands and their trajectories. Nevertheless, it was found that most of them are “cold”, between 60 and 100 °C. Only 117 firebrands had a temperature above 147 °C.

Different characteristics of the particles moving in the flow were obtained after processing the video data from the thermal imagers. Figure 6 shows the number of the particles versus the distance to the fire front.

Spread rates were obtained from fire isochrones created using the long-wave aerial IR imagery [8]. The isochrones were drawn by mapping the gradient of pixel intensity for each image and manually tracing a curve along the highest gradient. These were compared visually against the visible spectrum aerial imagery, and it was determined that this method was sufficiently accurate for determining the location of the leading edge of the fire front. By measuring the distances between fire isochrones in ArcGIS, it was possible to estimate spread rates. Knowing the position of IR cameras, fire front spread rate and time, we can calculate the distance from the fire front to IR cameras. The distance was calculated between nearest point of fire front line and IR cameras position.

Processing of infrared video showed that starting from a distance of 13 m from fire front, an increasing number of firebrands were observed in a

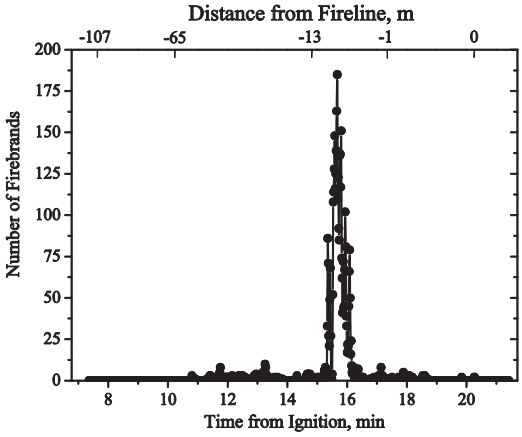

Fig. 6. Amount of particles versus the distance to the fire front.

controlled volume, increasing from only a few to 180 per second. At the same time, it is seen that the number of the particles is practically equal to zero at a distance of several meters before the fire front. This fact can be explained by the pre-burn removal of fuels on the plot to protect the equipment.

To use the obtained results in the mathematical models describing the propagation of wildland fires, we obtained relationships describing the time-variation of the number of particles that dropped on the pan-covered surface (1.4 m^2) and the number of particles that flew through the IR control volume (1 m^3). We considered a regression function for two variables: x, the time and y, the distance from the fire front to the thermal imager. The solution was obtained by using a nonlinear surface fitting and a Levenberg Marquardt iteration algorithm in the OriginPro software (OriginLab Corporation) for the number of particles that dropped on the studied surface per second (z) and the number of particles that flew through the control volume per second (z_1).

Finally, we obtain the equations as follows:

$$z = 0,11914 + 39,64119 \cdot e^{-e^{-\frac{x-939,7428}{14,13416}}} + 20,3029 \cdot e^{-e^{-\frac{y+9,40588}{0,33163}}} - 60,0536 \cdot e^{-e^{-\frac{x-939,7428}{14,13416}} - e^{-\frac{y+9,40588}{0,33163}}}, \quad (1)$$

$$z_1 = 0,75989 + 370,6615 \cdot e^{-e^{-\frac{x-935,2186}{11,69378}}} - 302,228 \cdot e^{-e^{-\frac{y+8,4769}{0,72778}}} - 68,7068 \cdot e^{-e^{-\frac{x-935,2186}{11,69378}} - e^{-\frac{y+8,4769}{0,72778}}}. \quad (2)$$

Comparing the experimental and calculated data (Eqs. (1) and (2)), we can conclude that these relationships allow us to describe the number of the dropped particles and the particles flying through the control volume per second with an acceptable accuracy. This is confirmed by the values of adj. R^2 0.74 and 0.86, respectively.

Figure 7 shows the effect of wind speed on the velocity of the flying particles.

Figure 7 clearly shows that the velocity of the particles depends on the wind speed. Between 10 and 20 min, the distribution of the maximum velocities has similar trends and magnitudes. We can assume that at low intensity surface fire the firebrands velocity follow by the ambient wind speed.

It can be seen from Fig. 8 that the increase in surface area of the particles leads to the decrease in average velocity. The maximum velocities are observed for the smallest particles. The velocities of the largest particles do not exceed 6 m/s. It is also seen that the particle velocity varies in the range of 0.1–10.5 m/s and the average velocity is 2.5 m/s.

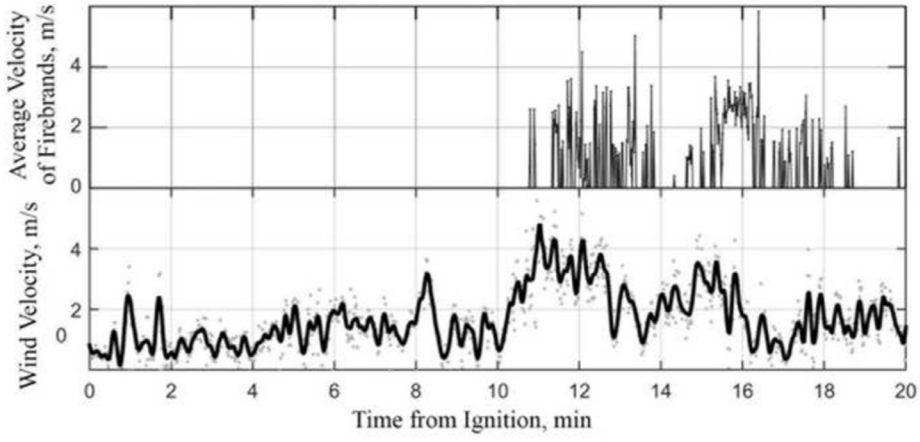

Fig. 7. Wind characteristics and average velocity of firebrands versus time.

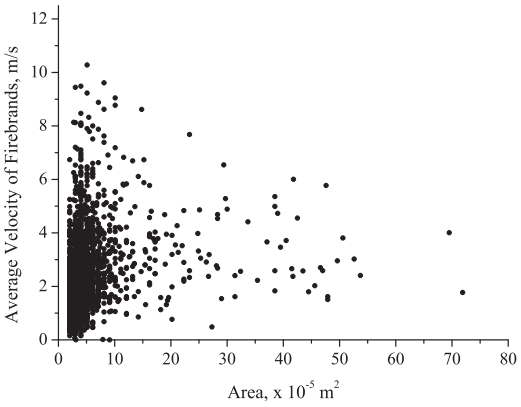

Fig. 8. Average velocity of the firebrands versus the surface area.

Analysis of the surface area of the particles has also shown that majority of the particles is in the range of $0–10\times10^{-5}$ m^2, which is 89% of the total number of the particles. This number is in good agreement with the observed data (76%, Fig. 5). At the same time, the number of the particles is similar to that on the curves in Fig. 5 and decreases with increasing the surface area.

4. Conclusion

Full-scale experiments were conducted to investigate the generation of firebrands during prescribed fires in the pine forests of New Jersey, USA (March 2013, 2014 and 2015). Several methods were tested to describe the generation of firebrands at the experimental sites. The firebrands were collected at three sites per fire and analyzed for mass and area distributions. Thermal image recording was used to measure the velocity, size, and number of the particles. The bark slices were found to be not less than 70% of collected particles and the remaining particles were pine and shrub branches. Most of the particles had a weight from 5 to 50 mg, with the majority observed in the range of 10–20 mg. About 80% of the firebrands were particles with an area of $(5–20)\times10^{-5}$ m^2. These results are in good agreement with observations from real fires [1]. The analysis of thermograms showed that an increase in number of the particles in a controlled volume was observed starting from 13 m ahead of the fire front and changed from several to 180 particles per second. Relationships describing the time-variation of the number of particles that dropped on a 1.4 m^2 surface and the number of particles that flew through a 1 m^3 volume were obtained. Comparing the experimental and calculated data (Eqs. (1) and (2)), we can conclude that these equations allow us to describe these two quantities with an acceptable accuracy (adj. R^2 0.74 and 0.86, respectively). In addition, the velocity of the particles was found to depend on the wind speed and an increase in particle area correlated to a decrease in average velocity.

Acknowledgments

This work was supported by the Joint Fire Science Program (JFSP, project #12-1-03-11), the Russian Foundation for Basic Research (projects #15-31-20314, #14-01-00211), the Tomsk State University Academic D.I. Mendeleev Fund Program and the Bushfire and Natural Hazard Cooperative Research Centre.

References

[1] S.L. Manzello, EI.D. Foote, *Fire Technol.* 50 (2014) 105–124.
[2] S.L. Manzello, T.G. Cleary, J.R. Shields, A. Maranghides, W.E. Mell, J.C. Yang, *Fire Saf. J.* 43 (3) (2008) 226–233.
[3] J.W. Mitchell, O. Patashnik, in: Fire and Materials Conference, The Tenth International Symposium of Fire and Materials', San Franscisco, CA (Interscience Communications: London, UK), 29.-31. January 2007.
[4] A. Maranghides, W.E. Mell, *A Case Study of a Community Affected by the Witch and Guejito Fires*, National Institute of Standards and Technology, 2009 Report No. 1635.
[5] J.P. Cohen, A Site-Specific Approach for Assessing the Fire Risk to Structures at the Wildland-Urban Interface, Report No. SE GTR-69, USDA Forest Service, 1991.
[6] P.J. Pagni, *Fire Saf. J.* 21 (1993) 331–340.
[7] V. Babrauskas, *Ignition Handbook*, Fire Science Publishers, Issaquah, 2003.
[8] M.E.L. Houssami, E. Mueller, A. Filkov, et al., *Fire Technol.* 52 (3) (2015) 731–751. http://dx.doi.org/10.1007/s10694-015-0492-z.
[9] K.L. Clark, N. Skowronski, M. Gallagher, *J. Sustain. For.* 34 (2015) 125–146.
[10] D. McKeown, J. Faulring, R. Krzaczek, S. Cavilia, J. van Aardt, in: Sylvia S. Shen, Paul E. Lewis (Eds.), Proceedings of SPIE Algorithms and Technologies for Multispectral, Hyperspectral, and Ultraspectral Imagery XVII, Vol. 8048, SPIE, Bellingham, WA, 2011.